EARTH SCIENCES
RESEARCH JOURNAL

Earth Sci. Res. J. Vol. 22, No. 2 (June, 2018): 129-138

UNIVERSIDAD NACIONAL DE COLOMBIA

SEDIMENTARY GEOLOGY

Diagenetic controls on reservoir quality of tight sandstone: A case study of the Upper Triassic Yanchang formation Chang 7 sandstones, Ordos Basin, China

Haihua Zhu[1,2*], Guangcheng Liu[1,2], DakangZhong[3], Tingshan Zhang[1,2], Jun Lang[1,2], JingliYao[4]

[1]Stake Key Laboratory of Oil and Gas Reservoir Geology and Exploitation, Chengdu 610500,China

[2]School of Geoscience and Technology, Southwest petroleum university, Chengdu 610500, China

[3]School of Earth Science, China University of Petroleum (Beijing), Beijing 102249, China

[4]Exploration & Development Research Institute of PetroChina Changqing Oil Field Company, Xi'an 710018, China

*Email of Corresponding Author:zhhswpu@163.com

ABSTRACT

Through a range of petrological techniques, the petrology, diagenesis, pore characteristics, and controlling factors on the regional variations of reservoir quality of the Chang 7 sandstones were studied. These sandstones, mainly arkoses, lithic arkoses, and feldspathic litharenites, were deposited in a delta front and turbidites in semi-deep to deep lacustrine. The detrital constituents were controlled by the provenance and sedimentary condition, which resulted in a spatially variable composition; e.g., high biotite and feldspar contents in the northeast (NE) of the study area, and high contents of rock fragments, especially dolomite, matrix, and quartz in the southwest (SW). Diagenesis includes intense mechanical compaction, cementation, and dissolution of unstable minerals. Diagenetic minerals which were derived internally include quartz, ankerite, ferrous calcite, albite, illite, kaolinite, and chlorite. Thus the original sandstone composition hadfirm control over the development and distribution of cement. Mechanical compaction and late-stage cementations contribute to the porosity loss of sandstones of Chang7 member. The dissolution porosity in major sandstone, slightly higher than primary porosity is principally dependent on the accessibility of acid fluid. The high content of plastic component facilitated the reduction of primary porosity and limited the mineral dissolution. The best reservoir sandstones are found in W, and partly from NE, M districts, with porosity are primary. The relatively high textural maturity of these sandstones reduces the impact of compaction on primary pores, and commonly existed chlorite rims limited the precipitation of pore filling quartz and carbonate cementation in late stage.

Keywords: Diagenesis; tight sandstone; reservoir quality; Ordos Basin

Controles diagenéticos en yacimientos de arenisca compacta: estudio de caso de las areniscas Chang 7, en la Formación Yanchang, Triásico Superior, cuenca de Ordos, China

RESUMEN

A través de una gama de técnicas petrológicas se estudió la petrología, la diagénesis, las características de poro y los factores que controlan las variaciones regionales de la calidad del yacimiento de las areniscas Chang 7. Estas areniscas, principalmente arcosas, arcosas líticas y arenitas líticas feldespáticas, se depositaron en un frente deltáico mientras las turbiditas se depositaron en ambientes lacustres profundos y semi-profundos. Los componentes detríticos dependen de la procedencia y la condición sedimentaria, lo que resultó en una composición variable en el espacio; por ejemplo, altos contenidos de biotita y feldespato en el noreste (NE) del área de estudio, y altos contenidos de fragmentos de roca, especialmente dolomita, matriz y cuarzo en el suroeste (SW). La diagénesis incluye compactación mecánica intensa, cementación y disolución de minerales inestables. Los minerales diagenéticos que se derivaron internamente incluyen cuarzo, ankerita, calcita ferrosa, albita, illita, caolinita y clorita. Por lo tanto, la composición original de arenisca tenía un firme control sobre el desarrollo y la distribución del cemento. La compactación mecánica y las cementaciones de la última etapa contribuyen a la pérdida de porosidad de las areniscas del miembro Chang7. La porosidad de disolución en la piedra arenisca principal, ligeramente más alta que la porosidad primaria, depende principalmente de la accesibilidad del fluido ácido. El alto contenido de componentes plásticos facilitó la reducción de la porosidad primaria y limitó la disolución del mineral. Las mejores areniscas de yacimiento se encuentran en los distritos Occidental, y en parte de los distritos Noroeste y Medio, con niveles primarios de porosidad. La madurez textural relativamente alta de estas areniscas reduce el impacto de la compactación en los poros primarios, y los bordes de clorito comúnmente existentes limitaron la precipitación del cuarzo de llenado de poros y la cementación de carbonato en la etapa tardía.

Palabras clave: Diagénesis; arenisca apretada, calidad del yacimiento; Cuenca de Ordos

Record
Manuscript received: 14/11/2017
Accepted for publication: 27/06/2018

How to cite item
Zhu, H., Liu, G., Zhong, D., Zhang, T., Lang, J., & Yao, J. (2018). Diagenetic controls on reservoir quality of tight sandstone: A case study of the Upper Triassic Yanchang formation Chang 7 sandstones, Ordos Basin, China. *Earth Sciences Research Journal*, 22(2), 129-138.
DOI:http://dx.doi.org/10.15446/esrj.v22n2.72251

1. Introduction

The tight oil produced from the Upper Triassic Chang 7 lacustrine sandstone accounts for 15% of the total oil and gas resources in the Ordos Basin of China and is considered an essential resource for future exploration (Zouet al.,2013; Asghar et al., 2018).The commercial production of tight oil requires significant hydraulic fracturing, similarly to production in shale gas. However low permeability and high heterogeneity of these sandstone reservoirs due to multi-source and variable sedimentary conditions, mean that oil production varies remarkably among different plays; e.g., only 40% of wells in the Changqing Oilfield gain commercial oil flow rates during formation testing after conventional fracturing (Duet al., 2014; Nawaz et al., 2018). Pore structure is critical for fluid accumulation and flows within reservoirs, and it controls the proportion of recoverable hydrocarbons as well as the results of hydraulic fracturing (Shanley & Cluff, 2015; Indan et al., 2018). Therefore, the prediction of reservoir quality and heterogeneity remains a crucial challenge for tight oil exploration and exploitation.

Porosity and permeability of sandstone reservoir quality is a function both of depositional conditions, which controlsfirst sediment composition, and diagenetic processes (Ajdukiewiczet al., 2010; Ozkanet al., 2011; Harith et al., 2018). The methods of diagenesis in sedimentary basins are generally well understood (Bjørlykke & Jahren, 2010; Bjørlykke & Jahren, 2012; Burley & Worden, 2003; Morad, 2009; Worden & Morad, 2009; Khawaj et al., 2018). However, there is uncertainty regarding a) whether the geochemical system is open or closed during diagenesis in sedimentary basins (Bjørkum & Gjelsvik, 1988; Bjørlykke & Jahren, 2010; Gluyas&Coleman, 1992; Sullivan et al., 1990; Worden & Barclay, 2000; Usman et al., 2018), and b) the origin and formation process of authigenic minerals, including clay minerals, and carbonate and quartz cements in sandstone (Barclay & Worden, 2000; Dowey, 2012;Worden & Morad, 2000). The Chang 7 sandstone is primarily fine-grained with extremely low permeability (typically <0.3 x 10^{-3} um^2). Mass transport in the sandstone was limited during the period of deep burial. Therefore the study of fine-grained sandstone helps to reveal the origins of authigenicminerals under relatively closed conditions. In this work, we address the following questions: (1) How did the original composition of the Chang 7 sandstone control the species of authigenic minerals in Ordos Basin? (2) How did the diagenetic process influence the quality of the tight oil reservoir?

2. Geological setting

The research area is located in the southwest of the Ordos Basin, covering an area of over 50,000 km^2, including the southern parts of the Yishan Slope and the Tianhuan Depression (Figure 1). The Triassic rocks in the study area include the Liujiagou, Heshanggou, Zhifang, and Yanchang formations, with the Liujiagou Formation being the lowermost unit. The Upper Triassic Yanchang Formation consists of 10 units from Chang 10 at the base to Chang1 at the top, which reflects the entire evolution of the basin from emergence to extinction (Deng et al., 2011; Naidu et al., 2018). The oil is generated mainly from the Chang 7_3 shales (35~40m) which were deposited during the period of highest lake level and were stored in next turbiditeand delta-front sandstones of Chang7_1~Chang7_2 with very fine to fine grain size and low permeability (Figure 2).

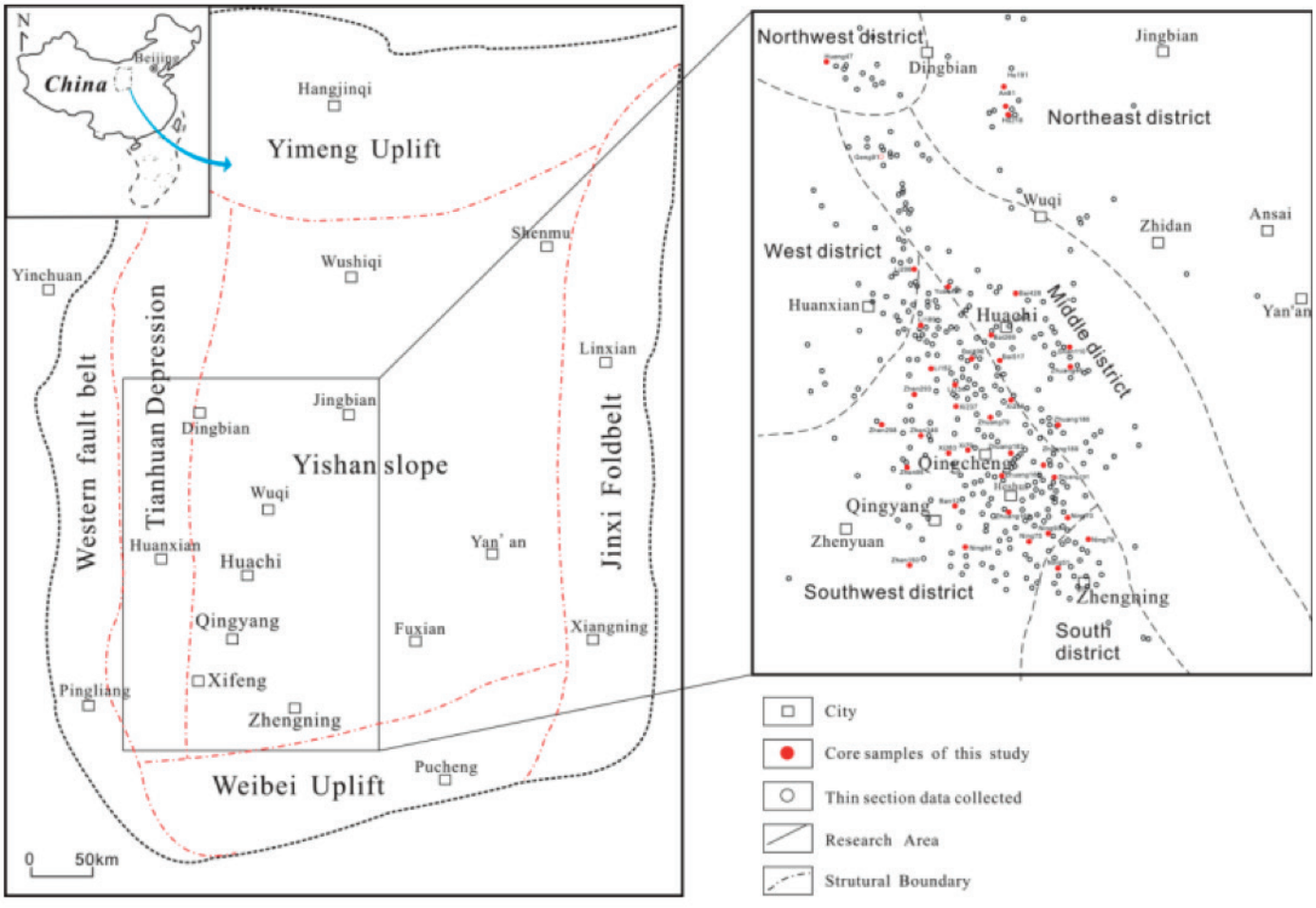

Figure 1. The study area in the southwest of Ordos Basin. The study area is divided into five districts with different provenances (Yang et al., 2010)

Yang et al. (2010) split the study area into South(S), West (W) Southwest (SW), Northeast (NE), Northwest (NE) and Middle/Central (M) areas with different provenances, according to the distribution of heavy and light mineral assemblages and the compositions of rock fragments. This scheme is adopted in the present study (Figure 1). The sediments were derived mainly from the basic volcanic and metamorphic rocks of the Yinshan Upland in the northeast of the Ordos Basin, and from the dolomite and acid volcanic rocks of the Qinlian Upland in the southwest (Xie, 2016; Yang et al., 2011; Barakat et al., 2018). The terrain slope of NE districts is gentle, and sandstones are mainly derived from braided river delta front, while in SW and M districts, sandstones deposited in meandering delta front and gravity flow are well developed(Yang et al., 2010; Sunny, 2018).

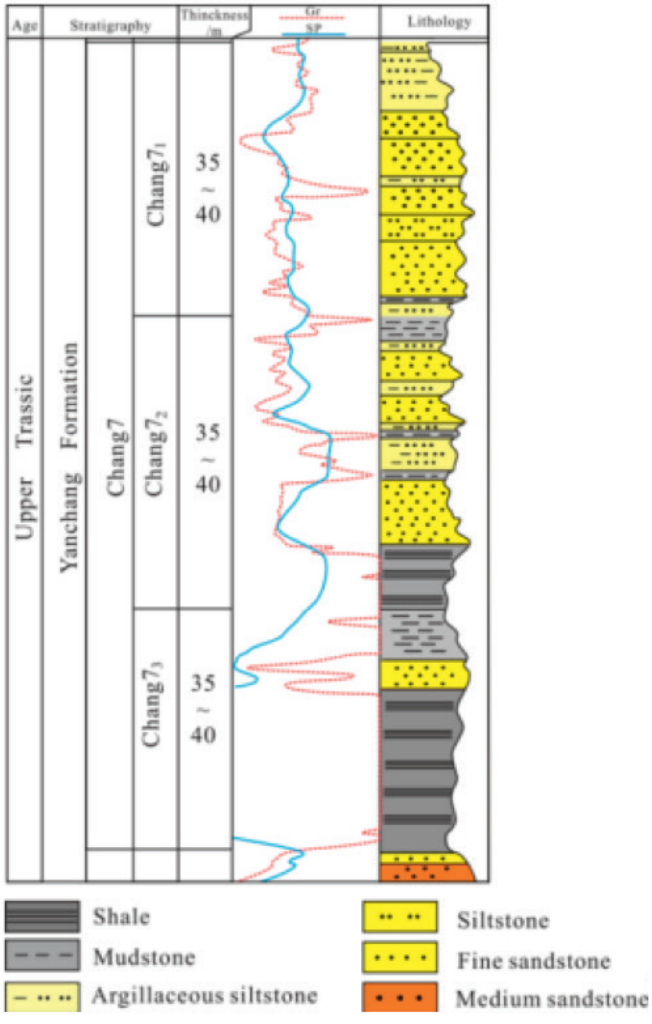

Figure 2. Generalized stratigraphy of the 7th Member (Chang 7) of Yanchang Formation, Ordos Basin

The Chang 7 section underwent rapid and continuous burial after initial deposition, with the maximum burial depth being ~4000 m in the SW of the basin and ~3000 m in the NE of the basin. Subsequently, the section was uplifted to its present burial depth of 1500 m to 2500 m during the Yanshan Orogeny in the Late Cretaceous and the Himalayan orogeny in the Cenozoic (Figure3).

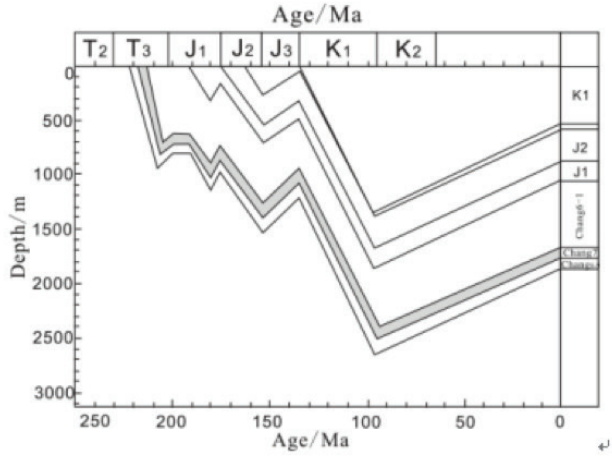

Figure 3. Typical burial process of Chang 7 member in the study area

3. Samples and methods

Fifty samples collected from study area were impregnated with resin before thin sectioning for porosity identification. Thin sections were stained with Alizarin Red S and K-ferricyanide for carbonate mineral determination. Texture and composition of these sandstones were determined under a petrographic microscope. Cathodoluminescence (CL) analysis of thin polished sections was carried out by a CITL Cold Cathode Luminescence 8200 mk5, excitation energy 20 kV, 400 mA.

The textural studies of the cement in the sandstone samples were performed on polished blocks and fractured surfaces, coated with gold on FEI Quanta 200F Scanning electron microscopy (SEM) equipped with an energy dispersive spectrometer and operated under 15–20 kV.The analyses were performed at the State Key Laboratory of Petroleum Resource and Prospecting, China University of Petroleum (Beijing).

PetroChina Changqing Oil Field Company provided additional point count data of 1493 thin sections from 361 wells, and helium porosity and permeability (6928 samples). The many thin section data provide an overall understanding of the distribution of detrital and cement minerals.

4. Results

4.1 Sandstone composition

The Chang 7 tight sandstone in the study area consists mainly of fine (0.125 mm) to very fine (0.065 mm) grained, moderate to well sorted, and poorly rounded arkoses, lithic arkoses, and feldspathic litharenites, according to the Folk's (1974) sandstone classification scheme (Figure 4).

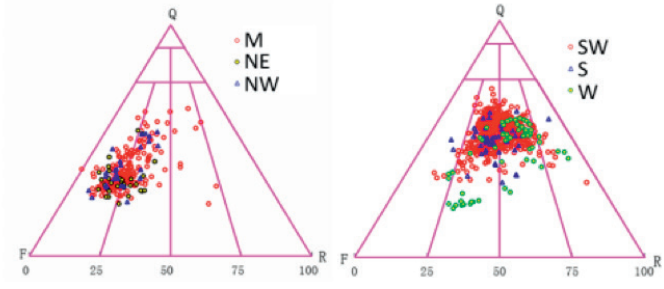

Figure 4. QFR classification of Chang 7 sandstone (after Folk, 1968). The ternary diagram shows the various types of Chang 7 sandstones with different sediment origins in different parts of the research area.

Point count data from 1513thin sections show that detrital quartz and feldspar are the most abundant minerals of both Chang7_1 and Chang 7_2 (Table 1).

Quartz is the most abundant mineral with contents ranges from 25%~41% with an average of 36% in Chang7$_1$, and 25%~40% with an average of 36% in Chang 7$_2$. Feldspar content of Chang 7$_1$ is 19%~39%, averaging 24% and 20%~43%, averaging 25% in Chang 7$_2$. Lithic grains were made up mainly by eruptive rock, quartzite, phyllite, and dolomite, and to a lesser degree from slate, aphanite, schist and metasandstone, and a small amount of limestone, high grain rock. The total content of lithic grains of Chang 7$_1$ ranges from 10%~23%, averaging 17%, and 12%~25%, averaging 18% of Chang 7$_2$. Lithic grains content of W, S, and SW districts are higher than that of NE and NW and are characterized by relatively abundant dolomite, phyllite, and quartzite. Mica is familiar throughout the basin, with a content range from 5%~13%, averaging 6% of Chang 7$_1$ and 3%~6%, averaging 5% of Chang 7$_2$.

The detrital composition shows little change vertically throughout the Chang 7 unit, but spatial differences are observed. E.g., Chang 7$_1$ sandstones from NE and NW districts are characterized by a relative higher content of feldspar and mica, and low quartz and lithic grains contrast with that of sandstones from S, W, and SW districts. And sandstones from Chang7$_2$ show the similar distribution pattern of detrital.

The matrix of the Chang 7 sandstone is mainly fine-grained minerals, mostly clay minerals that fill interstitial spaces amongst the framework grains. Matrix content of Chang 7$_1$ ranges from 7%~11%, averaging 10%, and 5%~12%, averaging 10% of Chang 7$_2$. The matrix contents in SW, S and M districts are higher than that in NE, NW and W districts (Table 2).

Table 1. Statistics of detrital components of Chang 7 member sandstones

Member	Districts	samples	quartz	chert	feldspar	Rock fragments contents	eruptive rock	aphanite	high grade rock	quartzite	schist	phyllite	Metasand stone	slate	Lime-stone	dolostone	mica	Other debris
Chang7$_1$	NE	33	25.08	0.27	39.04	12.52	2.38	0.77	1.46	1.63	0.55	1.88	0.73	0.82	0.03	0.78	7.84	1.44
	NW	27	27.50	0.17	34.25	10.49	1.69	0.60	1.25	1.01	0.43	1.67	0.43	0.75	0.00	0.24	12.79	2.39
	M	190	28.08	0.40	35.00	12.26	1.90	0.57	0.34	1.20	0.48	2.15	0.48	0.70	0.27	3.38	7.93	0.72
	S	47	38.12	0.29	21.27	18.46	1.93	1.13	0.48	2.30	1.13	3.53	0.79	1.32	1.26	3.49	6.32	1.04
	W	61	33.25	0.39	22.29	23.08	3.44	2.05	0.36	2.46	1.30	3.81	1.44	1.95	0.53	4.97	5.12	0.63
	SW	478	40.99	0.55	19.00	18.65	2.30	0.96	0.24	2.41	0.82	3.98	0.82	1.29	0.77	4.50	4.88	0.47
	Total	836	36.27	0.47	24.29	17.01	2.26	0.94	0.36	2.05	0.77	3.37	0.77	1.17	0.61	3.94	6.05	0.67
Chang7$_2$	NE	108	25.11	0.31	42.52	12.48	3.01	0.88	0.46	1.36	0.48	2.02	0.87	0.93	0.03	0.27	6.32	2.17
	NW	3	35.67	0.50	35.67	11.83	2.50	1.83	0.00	2.33	0.67	2.33	0.83	0.67	0.00	0.00	3.67	0.67
	M	45	25.80	0.50	33.90	14.01	2.02	0.68	0.66	1.43	0.38	2.02	0.32	0.71	0.50	3.67	6.34	1.58
	S	30	37.46	0.20	23.10	17.12	2.06	0.62	0.33	2.04	0.73	3.72	0.84	1.46	0.12	4.36	6.51	0.83
	W	35	33.08	0.56	24.33	24.92	4.19	1.99	1.18	2.89	1.45	3.57	1.30	2.55	0.59	4.33	3.16	0.85
	SW	486	40.16	0.49	19.68	19.39	2.35	1.19	0.26	2.45	0.87	4.02	1.02	1.29	0.59	4.58	4.85	0.65
	Total	707	36.45	0.46	24.54	18.13	2.51	1.13	0.36	2.22	0.80	3.54	0.96	1.26	0.47	3.82	5.16	0.96

Table 2. Statistics of matrix and cement composition of Chang 7 member sandstone

Member	Districts	samples	Matrix			Total Matrix	cement									Total Cements	Total interstitial material
			I	Ch	others		calcite	Fe-calcite	dolomite	ankerite	quatrz	feldspar	Ch-rims	K	others		
Chang7$_1$	NE	33	1.81	3.69	0.38	5.88	0.18	4.67	0.00	0.74	1.17	0.13	0.00	1.92	0.54	9.35	15.22
	NW	27	2.10	2.43	0.33	4.86	0.00	5.19	0.00	0.20	1.03	0.11	0.30	2.97	0.42	10.22	15.06
	M	190	8.38	0.68	0.32	9.38	0.42	1.95	0.11	2.63	1.07	0.12	0.11	0.26	0.23	6.9	16.28
	S	47	10.32	0.66	0.01	10.99	0.17	1.77	0.00	1.52	0.86	0.04	0.00	0.00	0.09	4.45	15.43
	W	61	8.18	1.22	0.00	9.4	0.21	1.32	0.00	3.10	1.33	0.06	0.00	0.05	0.25	6.32	15.74
	SW	478	10.13	0.21	0.02	10.36	0.14	1.72	0.02	2.04	1.06	0.05	0.03	0.07	0.37	5.5	15.86
	Total	836	9.01	0.63	0.11	9.75	0.21	1.98	0.04	2.11	1.07	0.07	0.05	0.27	0.32	6.12	15.87
Chang7$_2$	NE	108	3.04	3.42	0.18	6.64	0.14	3.71	0.00	0.46	0.78	0.15	0.01	1.37	0.08	6.62	13.27
	NW	3	1.33	0.00	0.00	1.33	0.00	3.50	0.00	0.00	4.00	0.50	0.00	3.33	0.00	11.33	12.67
	M	45	6.47	1.86	3.05	11.38	0.11	2.40	0.04	3.13	0.95	0.10	0.00	0.10	1.09	7.92	19.32
	S	30	11.58	0.03	0.00	11.61	0.00	1.41	0.00	1.12	0.95	0.04	0.00	0.00	0.41	3.93	15.54
	W	35	5.53	2.61	0.01	8.15	0.09	1.35	0.11	1.48	1.35	0.06	0.00	0.95	0.28	5.67	13.82
	SW	486	9.20	0.40	0.08	9.68	0.23	1.53	0.01	2.10	1.18	0.06	0.00	0.10	0.38	5.59	15.29
	Total	707	7.96	1.05	0.28	9.29	0.19	1.92	0.02	1.83	1.12	0.07	0.00	0.35	0.38	5.88	15.16

4.2 Diagenetic minerals

The diagenetic minerals in Chang 7 sandstone are mainly included Fe-calcite, ankerite, quartz followed by minor calcite, dolomite, albite, kaolin, and chlorite rims. Total diagenetic minerals content of Chang71 range from 4%~10%, averaging 7% and 4%~11%,averaging 7% of Chang72. Samples from NE, NW and M districts contain higher cement content than that of sandstones from W, S and SW area.

4.2.1 Quartz cement

Quartz cement, which ranges in average abundance from 0.9% to 1% (average of 1%) in Chang71 and mainly 0.8%~1.4% (average of 1.1%) in Chang72, occurs as either euhedral quartz crystals that fill intergranular or dissolution pores or as syntaxial overgrowths around quartz grains.

Two generations of quartz cement can be distinguished. First generation quartz cement is covered by chlorite rims and filling primary pores (Figure5a). Second generation quartz cement grew over the chlorite rims and occurred as small euhedral or pyramidal quartz crystals filling primary and dissolution pores (Figure5b). Quartz cement iscommon in coarser sandstones with fewer matrix present.

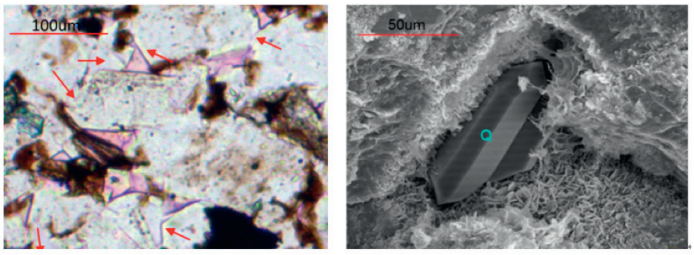

Figure 5. Quartz cement in Chang 7 sandstones. A: early quartz overgrowth been covered by and thus predate chlorite rim, Well Wu 62, 1827.06m. B: authigenic quartz in the intergranular pore, postdate chlorite rims in SEM picture, Well Gao 38, 2125.46m.

4.2.2 Carbonate cement

The amount of carbonate cement varies from 3% to 6%, averaging 4% in Chang7_1 and Chang7_2, and includes Fe-calcite, ankerite, and minor calcite (~0.2%) and dolomite (generally <0.1%).

Calcite is stained red in thin section and bright yellow under cathodoluminescence (CL). Two generations of calcite are recognized: calcite I fill large intergranular pores as poikilotopic crystals (>100um) between uncompacted detrital grains. Calcite-II partly or entirely replaces detrital grains and be engulfed by Fe-calcite (Figure 6). Although the content of calcite cement is up to 40%, it is commonly absent and has a mean content of 0.2%.

The Fe-calcite is stained purple or blue-violet and dark orange under CL with content ranges from 2%~6%, averaging 2% in Chang 7_1, and from 1%~4%, averaging 2% in Chang 7_2. The Fe-calcite is most abundant in the NE, NW districts (> 3.5%) and decreases to < 2% in the SW, S and W districts. It usually occurs as micro- to coarse-crystalline (10~100μm) cement that partly or wholy fills isolated intergranular pores, engulfing quartz overgrowth, chlorite rims and calcite(Figure 6, Figure 7a).

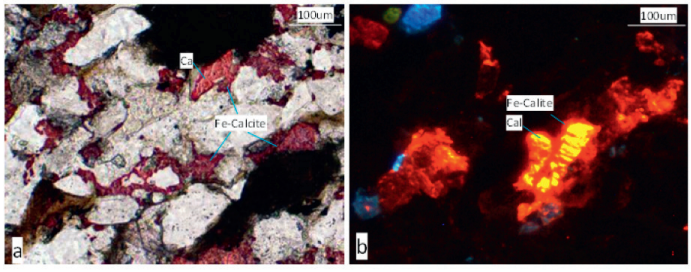

Figure 6. Calcite-II partly or entirely replaces detrital grains and be engulfed by Fe-calcite under polarizing microscope and CL

Ankerite, stained wathlet blue under the thin section, is micro- to coarse-crystalline (<10~100μm) and generally occurs as overgrowths around dolomite grains, Fe-calcite, and dolomite cement filling intergranular and dissolution pores (Figure7b). Contrary to the distribution of calcite, ankerite cement mainly occurs in samples from M, S, W, and SW districts with contents ranging from 1%~3% in Chang7_1 and Chang 7_2. And minor ankerite is found in NE and NW districts (0~1%).

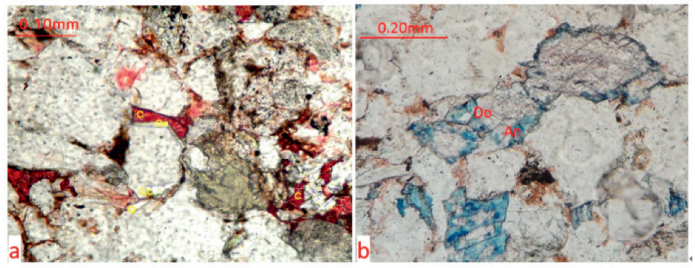

Figure 7. Fe-carbonate cement in Chang 7 sandstones under thin section. (a): Fe-calcite grows over quartz overgrowth, Intergranular pores mostly filled by quartz and Fe-calcite, Well Ning 31, 1654.47m. (b): ankerite occurs as overgrowth of dolomite grains and filling the intergranular residue pores after quartz cement and compaction, Well Li 45, 2276.02m.

4.2.3 Clay cement

Clay cement identified in the studied sandstones include chlorite, kaolin, and illite.

Kaolin is mostly present in the samples from NE and NW districts with contents ranges from 1.9%~3.0% of Chang 7_1 and 1.4%~3.3% of Chang 7_2. Little kaolin is found in samples from M, S and SW areas. It occurs as thin stacks of pseudo-hexagonal plates filling the primary pores and feldspars dissolution pores and partially entrapped by chlorite (Figure 8).

Authigenic chlorite occurred in the Chang 7 sandstone as two forms: grain rims and pore-filling. Grain rims chlorite found in about 15% of total samples are thin (3-10μm) and discontinuous with crystals orient perpendicular to the surface of detrital and authigenic quartz crystals (Figure 9). When present, it makes up <0.30% of the whole rock volume. The thickness of chlorite rims on authigenic quartz crystals is much thinner than that on the detrital grains. Chlorite is often observed to wholly or partly completely replace biotite, and in places, its content can be up to ~20% of the whole rock volume.

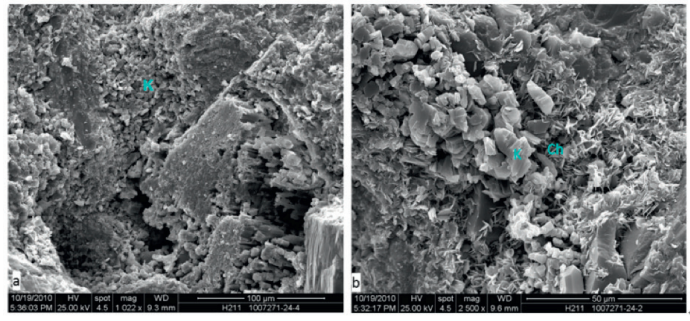

Figure 8. Diagenetickaolin in Chang 7 sandstones. a) kaolinite plates filling the primary pores, Well Hu 211, 2300.4m; b) kaolin with pseudo-hexagonal plates grows over and postdate by chlorite coating, Well Hu 211, 2300.4m.

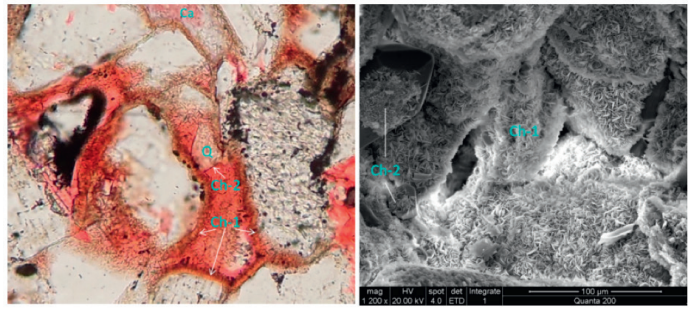

Figure 9. Chlorite rims on detrital (Ch-1) and diagenetic quartz (Ch-2) surface. The chlorite rims on authigenic quartz crystals are much thinner than that on the detrital grains. a) well Gao18,1917.8m and b) well Huan 54,2661.2m.

Illite mineral occurs in every sample with three forms under SEM: i) flaky and honeycomb-like crystal with spiny terminations tangentially coating detrital grains (Figure 10a); ii) flaky filaments filling intergranular pores (Figure 10b-e); and iii) fibrous, hair-like illiteoccurring as pore-bridging cement or filling dissolution pores (Figure 10f). And most of the illite occurs as the first two forms. Fibrous illite is rare in Chang 7 sandstones.

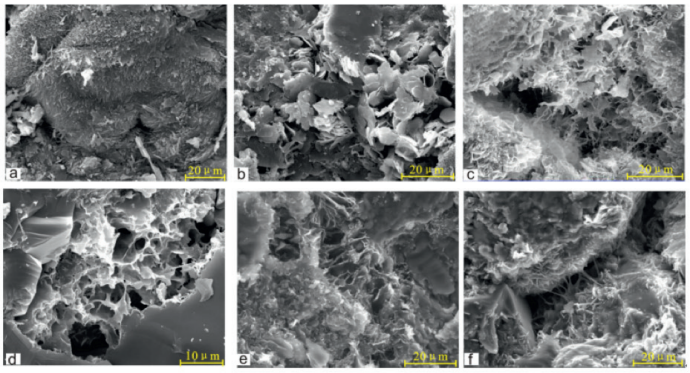

Figure 10. The illite minerals with different crystal shapes of Chang 7 sandstones. (a) flaky illites covering the detrital grains, well Geng 292, 2481.01m; (b) flaky illites disorderly filling the intergranular pores, well Geng 292,2481.01m; (c) flaky to hair-like illite partly filling the intergranular pores, well Huan 54, 2650m; (d) Honeycomb illite covering the detrital grains, well An72, 2237.43m; (e) illite with no significant crystalline morphology, well Zhuang40, 1824.16m; (f) pore-bridging silk-thread illite, well Gao 38, 2125.46m.

Table 3. Statistics of thin section porosity of Chang 7 member sandstones (%)

Member	Samples	Districts	Total porosity	Intergranular porosity	Dissolution porosity(%)			Intracrystalline porosity	Microcrack
					Feldspar	Rockfragment	Cements		
Chang7_1	NE	33	2.3	1.4	0.6	0.1	0.0	0.1	0.1
	NW	27	1.9	0.7	1.2	0.1	0.0	0.0	0.1
	M	190	1.7	0.8	0.7	0.1	0.1	0.0	0.0
	S	47	1.9	0.6	1.0	0.2	0.1	0.0	0.0
	W	61	4.7	3.5	0.7	0.2	0.0	0.0	0.0
	SW	478	1.5	0.4	0.8	0.1	0.1	0.0	0.0
	Total	836	1.9	0.8	0.8	0.1	0.1	0.0	0.0
Chang7_2	NE	108	2.3	1.1	1.1	0.1	0.0	0.0	0.0
	NW	3	0.7	0.0	0.5	0.0	0.0	0.2	0.0
	M	45	2.0	1.1	0.7	0.1	0.0	0.1	0.1
	S	30	1.6	0.3	1.1	0.1	0.0	0.0	0.0
	W	35	4.9	3.3	1.0	0.3	0.2	0.0	0.2
	SW	486	2.0	0.7	1.0	0.1	0.1	0.0	0.0
	Total	707	2.1	0.9	1.0	0.1	0.1	0.0	0.0

4.4. Porosity and permeability

Average porosity of thin sections from different districts ranges from 1.7%~4.7% and averages 1.9% in Chang 7_1 and from 0.7%~4.9%, averages 2.2%in Chang72 (Table 3). Highest thin section porosities are found in samples from W, NE districts with porosity up to 4.9%.

Thin section and SEM analyses show that there are three types of pores: intergranular pores, which make up a substantial amount of the total porosity (0.4%~3.5%, av.0.8% in Chang 7_1 and 0.3%~3.3%, av.0.9% in Chang 7_2); secondary pores (0.7%~1.3%, av.1.0% in Chang 7_1 and 0.8%~1.4%, av.1.2% in Chang 7_2) and micropores. Secondary pores are mostly formed by the dissolution of feldspar and a small number of rock fragments and carbonate cement. The micropores with a pore radius of 0.5 μm or less (Pittman, 1971; Jefrin et al., 2018) can be of primary or secondary origin (Loucks & Dutton, 2007), and are associated with the clay minerals and weathered or altered rock fragments.

Although microporosity cannot be quantified in thin section, it is an important pore type of Chang 7 sandstones. The scatter plot of thin section porosity, core plug porosity versus depths shows that the thin section porosity variation trends with depth are overall in agreement with that of core plug porosity (Figure11). Whereas the point count thin section porosity (mainly macropores) is significantly less than core plug porosity (0.9%~20.4%, av.9.3% in Chang 7_1 and 01.4%~19.5%, av.9.6% in Chang 7_2) indicating that abundant micropores in the Chang 7 sandstones are not counted in thin section.

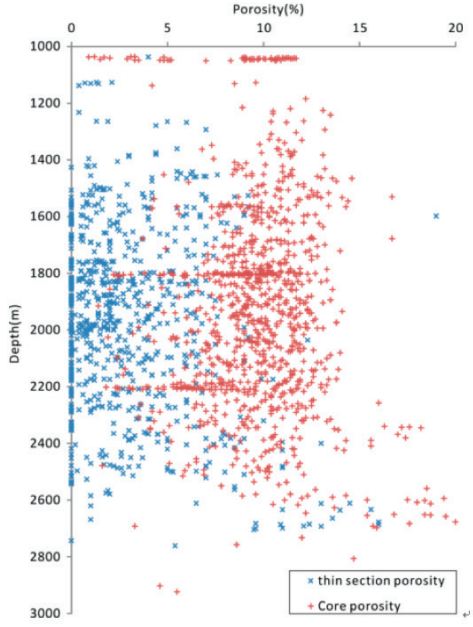

Figure 11. Plots of thin section porosity, core porosity versus depth

5. Discussion

5.1. Paragenetic sequence

The main diagenetic processes affecting Chang 7 sandstones include mechanical compaction, cementation of quartz, Fe-calcite and ankerite and authigenesis of chlorite, kaolin, and illite.

Grain-coating clay formed on detrital grain surfaces in Chang 7 sandstones occur as flaky texture, tangentially arranged around, and are typically originated by postdepositional infiltration (Matlack et al., 1989).

Dominantly long and concavo-convex contacts combine with flexible grain deformation in Chang 7 sandstones, suggests a moderate to intense mechanical compaction. In sandstones containing significant content of

ductile components, mechanical compaction is characterized by grain rearrangement and plastic grain deformation at relatively shallow depths (Pittman and Larese, 1991).

Quartz cement (>1%) are standard in Chang 7 sandstones and have several sources (McBride, 1989; Worden and Morad, 2000; Hussin et al., 2017). The presence of syntaxial quartz overgrowth near the sites of intergranular dissolution and on tightly packed detrital quartz grains indicates a mesogenetic origin (McBride, 1989; Sibley & Blatt, 1976; Worden &Morad, 2000; Sunny et al., 2018). In Chang 7 sandstones, concavo-convex contacts between detrital quartz are widely observed. It seems that in situ pressure solution provide materials for the bulk of the cement. No apparent correlations are found between average contents of detrital contents with quartz cement indicating that: 1) the silica sources, including the situ pressure solution of quartz, feldspar dissolution, and smectite illitization, exceed the demand for quartz precipitation in Chang 7 sandstone; and 2) the available pore space for silica precipitate and temperature as well as pH condition are more important factors for quartz cement.

Diagenetic chlorite can have multi origins but typically forms at relativelyhigh temperatures (Spoetlet al., 1994). Chlorite may form by (i) the alteration of eogenetic, grain-coating berthierine or odinite (Hillier & Velde 1992; Humphreys et al., 1989; Kugler & McHugh, 1990), kaolinite and smectite precursor in deltaic deposits (Ehrenberg, 1993; Ryan, 1997; Stokkendal et al., 2009); (ii) by the dissolution of Fe- and Mg-rich detrital grains (Anjos et al., 2000; Blackbourn & Thomson, 2000; Ros et al., 1994; Remy, 1994; Valloni et al., 1991). Diagenetic chlorites in Chang 7 sandstones were most probably formed by (i) massive biotite alteration, (ii) the transformation of precursor clay, and (iii) direct precipitation from pore fluids. Petrographic examination showed that authigenic chlorite, especially pore filling chlorite, is often related to degradingbiotite (Figure12) and, accordingly, high authigenic chlorite contents are associated with biotite-rich sandstones. The chlorite-coats grow both on detrital and diagenetic quartz surface with different thickness (Figure 9), and when present on detrital grains, the chlorite coating is thicker than that of the diagenetic quartz, indicating that chlorite coating on diagenetic quartz is direct precipitates from pore water, while chlorite on detrital grain probably is firstly transformed from precursor clay coating and then continue to grow as thicker rims.

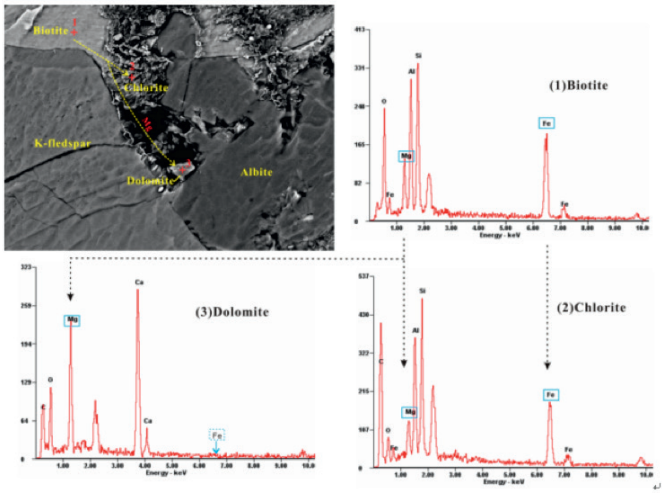

Figure 12. Biotite alteration and associated products. Biotite altered to chlorite and dolomite by releasing magnesium, well Zhuang191, 2498.6m.

The positive correlation of high-grade metamorphic rock fragments (HMRFs) versus chlorite contents reflects that the HMRFs could be the additional source of ions for the chlorite rims (Figure13).

Diagenetic kaolin usually occurs in mesogenetic stage and mostly occurred in NE and NW districts where sandstones contain abundant feldspar. SEM observations showed that kaolinite filling the dissolution and intergranular pores and, thus, likely formed by the alteration of detrital feldspars. The formation of kaolinite would require acidic pH condition and sufficient Al and Si. The acidic fluids may have been derived from adjacent shales during the maturation of organic matter (Surdamet al., 1984). Negative correlations between matrix content, mainly illite, versus kaolin and other cement contents suggesting that precipitation pores, which are closely related with matrix content of sandstone, are essential for diagenetic kaolin (Figure 13a).

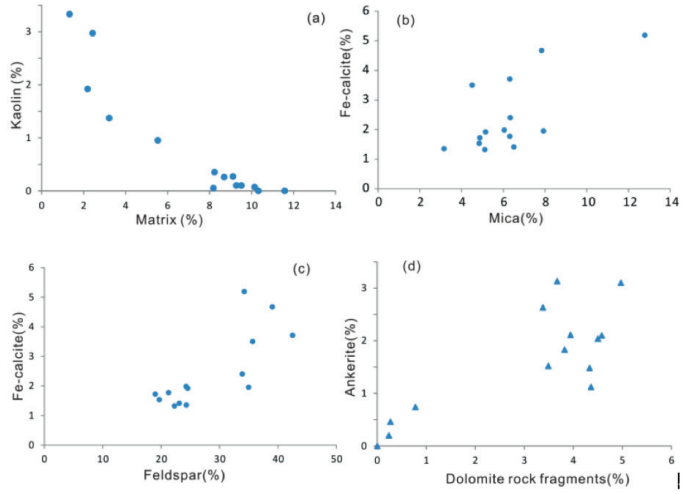

Figure 13. Content scatterplots of (a) matrix with kaolin, (b) mica with Fe-calcite, (c) feldspar with Fe-calcite and (d) dolomite rock fragments with ankerite.

The flaky and honeycomb-like illite is wide spreading in the Chang 7 sandstones, indicating that illite contains smectite mixed-layer. The presence of grain coating, flaky and honeycomb-like illite crystals with sharp edges suggest a diagenetic origin (Lemon & Cubitt, 2003; Moradet al., 2000). The extensive illitizaiton of smectite depend on high temperatures (90–130ºC) and sufficient K supply (Bjørlykke, 1998; Ehrenberg, 1993; Moradet al., 2000; Morad & De Ros, 1994). The K and Al ions needed for illite precipitation may have been derived from the feldspar dissolution.

Authigenic carbonates in Chang7 sandstones occur as micro to coarse crystalline poikilotopic, pore-filling blocky and isolated pore-filling, indicating precipitation in different stages.

The early calcite cement occupies an intergranular grain volume (IGV) of ~40% and blocks large intergranular pores between loosely packed detrital grains indicating it occurred before intense mechanical compaction.

The Fe-carbonate cement typically occurs as isolated pore filling, engulfing and thus postdating quartz overgrowth, chlorite rims, and calcite cement and were mainly formed at moderate to a deeper depth and have a mesogenetic origin. Homogenization temperatures of fluid inclusions reveal that the precipitation of Fe-carbonate cements at temperatures of 70ºC~150ºC and mainly focused on 100ºC~110ºC(Zhuet al., 2015).

Positive correlations between feldspar and mica versus Fe-calcite (Figure 13b-c) suggest that feldspar acid dissolution and mica alteration provided the bulk of Fe and Ca ions for late-stage Fe-calcite precipitation. Wang reported that light $\delta^{13}C$ PDB values (-8.02‰ ~ -3.23‰) in Fe-calcite (Wang et al., 2007), indicating carbon of Fe-calcite was most likely originated from the maturation of organic matter during burial process (Morad, 1998).

Whereas evident correlation of diagenetic ankerite with dolomite rock fragments proposes dolomite grains is likely to be the primary source for ankerite cement (Figure 13d). This is consistent with the heavier δ13C PDB values (-1.92‰ ~ -0.84‰) in ankerite, which indicating dolomite rock fragments may serve as the chief carbons source for later ankerite precipitation.

The relative timing of diagenetic minerals of sandstones of the Chang 7 member in the study area was inferred from the textural relationship as observed from thin section, SEM and a paragenetic sequence is present in Figure 14.

Diagentic Sequences	Early Late
Grain coating illite	
Mechanical compaction	
Early poikilotopic calcite cement	
Feldspar dissolution	
Authigenic albite	
Quartz cement	
Authigenic chlorite	
Authigenic kaolin	
Authigenic illite	
Fe-calcite cement	
Ankerite cement	

Figure 14. Diagenetic sequences of sandstones of Chang 7 members, Ordos basin

Sandstone reservoir quality is a function both of the depositional conditions and diagenetic processes (Ajdukiewicz et al., 2010).

The effect of mechanical compaction on the Chang 7 sandstones is evidenced by concavo-convex contacts and the deformation of micas and plastic grains. A plot of IGV versus cement volume indicates that compaction contributed to the major primary porosity loss of Chang 7 sandstones (Figure 15). Fine grain size, abundant mica, plastic grain as well as clay minerals, and rapid burial after deposition all contributed to compaction of the sandstone.

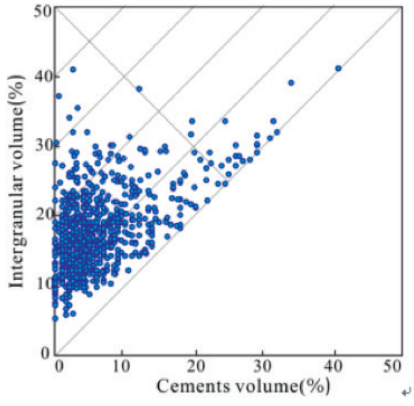

Figure 15. The plot of intergranular volume (%) versus cement (%) for the Chang 7 member sandstones, Ordos Basin (after Houseknecht, 1987)

Authigenic minerals, especially illite, quartz and carbonate minerals occupy an average of ~6% rock volumes and also played an essential role in further reducing porosity.

Carbonate cement, mainly Fe-calcite and ankerite, are the significant cement during the late stage, and these fill the residual intergranular and dissolution pores. The contribution of illite to the reduction in reservoir quality, by filling pore space and blocking pore throats (Worden & Morad, 2009), is more significant for fine sandstones than coarse sandstones (Armitage et al., 2010). Quartz overgrowth is avital reservoir quality reducing factor for many deep burial reservoirs (Worden & Morad, 2000). However, the influence of silica and albite cement on reservoir quality is limited due to their scarcity in Chang7 sandstone.

Though the very low reservoir porosity, thin section porosity of most Chang7 sandstones is still largely secondary (>50%) and thus is mainly controlled by the accessibility of acid fluid. Acidic fluids generated from the maturation of organic matter within the underlie Chang7_3 shales can directly migrate into the sandstones of Chang 7_2, then Chang7_1 generate generally upward decreasing of dissolution pores (Table 3).

No apparent correlation is found between feldspar content and dissolution porosity, but high content of plastic component, especially mica and clay minerals facilitate the reduction of primary porosity and permeability during compaction and make acid fluids accessing to sandstone difficult. Sandstones from M districts, where thickest source rock developed, contain lower dissolution porosity than that of other areas due to the high matrix and mica contents.

The best reservoir sandstones with relatively high core testing porosities (10%~20%)mainly distribute in W district and at depth ranges of 2300m–2800 m (Figure 16). These sandstones porosities are primary and show relatively coarse-grained, lower matrix and well preserved primary pores. And thus reservoir quality is mainly dependent on the textural maturity of the sandstones, controlled principally by depositional conditions (Tucker, 2003).

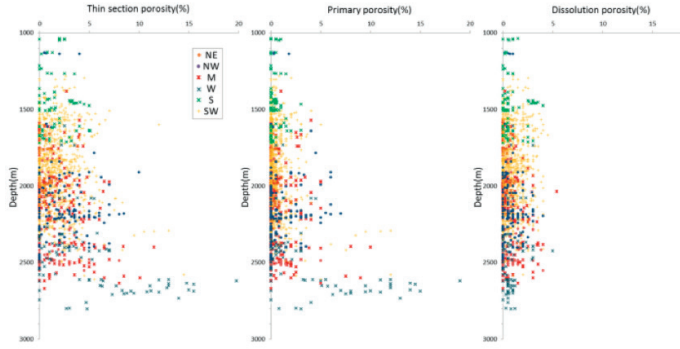

Figure 16. Distribution of thin section porosity, primary porosity and dissolution porosity with the depth of Chang 7member sandstones, Ordos basin.

These sandstones with well-preserved primary pore, from W, NE and M districts, are also characterized by chlorite coating and restively low quartz and carbonate cement (Figure 17). It is considered that chlorite coating improves reservoir quality in most cases, especially in deeply buried sandstones (Dowey, 2012; Ehrenberg, 1993; Tayloret al., 2010; Worden & Morad, 2009). The presence of chlorite coating inhibits quartz overgrowth, as well as carbonates cement by changing the grain surfaces to be oil wetting and preventing the access of water to detrital surfaces, thus stopping cementations (Al-Ramadan et al., 2004).

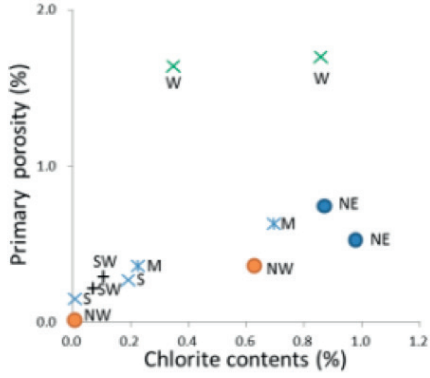

Figure 17. Scatter plots of chlorite contents (including pore filling chlorites and chlorite rims) versus primary porosity of Chang 7 member sandstone, Ordos basin

6 Conclusions

(1) The Upper Triassic Chang 7 sandstones are essential tight oil reservoirs with average porosity of 10.1% and average permeability of 0.18 × 103 μm2. They were deposited as delta front and semi-deep to deep lacustrine facies, producing a fine-grained, well-sorted, poorly rounded sandstone with a high matrix content. The detrital components were controlled by sediment provenance and are regionally distributed, with high biotite and feldspar contents in the NE and NW districts, and high contents of dolomite rock fragments and quartz in the SW, S, W districts.

(2) The diagenetic evolution of the Chang 7 sandstone is characterized by intense mechanical compaction and low cement content, especially low contents of quartz cement. The major authigenic minerals originated mainly from internal detrital alteration of sandstones and included quartz, ankerite, Fe-calcite, albite, illite, kaolinite, and chlorite. The composition of the original sandstone was the central control on the development of cement.

(3) The dissolution of feldspar is common despite intense mechanical compaction and is principally dependent on the accessibility of acid fluid. The best reservoir sandstones are found in W, and partly from NE, M districts, with porosity are primary. The relatively high textural maturity of these sandstones reduces the impact of compaction on primary pores, and commonly existed chlorite rims limited the precipitation of pore filling quartz and carbonate cementation in late stage.

Acknowledgments

We acknowledge PetroChina Changqing Oil Field Company for providing data including the results of thin section and core analyses. We are also grateful to the State Key Laboratory of Petroleum Resource and Prospecting at China University of Petroleum (Beijing) for providing testing equipment. This work was supported by a General Financial Grant from the China Postdoctoral Science Foundation (2015M580797) and by the Young Scholars Development Fund of Southwest Petroleum University, Chengdu, China (201499010046).

Reference

Ajdukiewicz, J. M., Nicholson, P. H., & Esch, W.L. (2010). Prediction of deep reservoir quality using early diagenetic process models in the Jurassic Norphlet Formation, Gulf of Mexico. AAPG Bulletin, 94(8), 1189-1227.

Al-Ramadan, K. A., Hussain, M., Imam, B., & Saner, S. (2004). Lithologic characteristics and diagenesis of the Devonian Jauf sandstone at Ghawar Field, Eastern Saudi Arabia. *Marine & Petroleum Geology*, 21(10), 1221-1234.

Anjos, S. M. C. D., Ros, L. F. D., Souza, R. S. D., Silva, C. M. D. A., & Sombra, C.L. (2000). Depositional and diagenetic controls on the reservoir quality of Lower Cretaceous Pendencia sandstones, Potiguar Rift Basin, Brazil. *AAPG Bulletin*, 84(11), 237-248.

Armitage, P. J., Worden, R. H., Faulkner, D. R., Aplin, A. C., Butcher, A. R., & Iliffe, J. (2010). Diagenetic and sedimentary controls on porosity in Lower Carboniferous fine-grained lithologies, Krechba field, Algeria: A petrological study of a caprock to a carbon capture site. *Marine & Petroleum Geology*, 27(7), 1395-1410.

Barclay, S. A., & Worden, R. H. (2000). Geochemical modelling of diagenetic reactions in a sub-arkosic sandstone. *Clay Minerals*, 35(1), 57-57.

Bjorkum, P. A., & Gjelsvik, N. (1988). An isochemical model for formation of authigenic kaolinite, K- feldspar and illite in sediments. *Journal of Sedimentary Petrology*, 58(3), 506-511.

Bjørlykke, K. (1998). Clay mineral diagenesis in sedimentary basins — a key to the prediction of rock properties. Examples from the North Sea Basin. *Clay Minerals*, 33(1), 15-34.

Bjørlykke, K., & Jahren, J. (2010). *Sandstones and Sandstone Reservoirs*. Petroleum Geoscience, Springer Berlin Heidelberg, pp. 113-140.

Bjørlykke, K., & Jahren, J. (2012). Open closed geochemical systems during diagenesis in sedimentary basins: Constraints on mass transfer during diagenesis and the prediction of porosity in sandstone and carbonate reservoirs. AAPG Bulletin, 96(12), 2193-2214.

Blackbourn, G. A., & Thomson, M. E. (2000). Britannia field, UK North Sea: petrographic constraints on Lower Cretaceous provenance, facies and the origin of slurry-flow deposits. *Petroleum Geoscience*, 6(4), 329-343.

Burley, S. D., & Worden, R. H. (2003). *Sandstone diagenesis: recent and ancient*. International Association of sedimentologists.

Deng, X., Fu, J., Yao, J., Pang, J., & Sun, B. (2011). Sedimentary facies of the Middle-Upper Triassic Yanchang Formation in Ordos Basin and breakthrough in petroleum exploration. *Journal of Palaeogeography*, 13(4), 443-455..

Dowey, P. (2012). *Prediction of clay minerals and grain-coatings in sandstone reservoirs utilising ancient examples and modern analogue studies*. University of Liverpool.

Ehrenberg, S. N. (1993). Preservation of anomalously high porosity in deeply buried sandstones by grain-coating chlorite: Examples from the Norwegian Continental Shelf. *AAPG Bulletin*, 77(7), 1260-1286.

Gluyas, J., & Coleman, M. (1992). Material flux and porosity changes during sediment diagenesis. *Nature*, 356(6364), 52-54.

Hillier, S., & Velde, B. (1992). Chlorite interstratified with a 7 Å mineral: an example from offshore Norway and possible implications for the interpretation of the composition of diagenetic chlorites. *Clay Minerals*, 27(4), 475-486.

Humphreys, B., & Humphreys, S. A. S. (1989). The distribution and significance of sedimentary apatite in Lower to Middle Devonian sediments East of Plymouth Sound. *Geoscience in South-West England*, 7(2).

Kugler, R. L., & Mchugh, A. (1990). Regional diagenetic variation in norphlet sandstone: implications for reservoir quality and the origin of porosity. *AAPG Bulletin*, 74, 9(9).

Lemon, N. M., & Cubitt, C. J. (2009). Illite Fluorescence Microscopy: A New Technique in the Study of Illite in the Merrimelia Formation, Cooper Basin, Australia. *Clay Mineral Cements in Sandstones*.

Loucks, R. G., & Dutton, S. P. (2007). *Importance of Micropores in Deeply Buried Tertiary Sandstones along the Texas Gulf Coast*. In: American Association of Petroleum Geologists Annual Convention Abstracts, 84.

Matlack, K. S., Houseknecht, D. W., Applin, K. R. (1989). Emplacement of clay into sand by infiltration. *Journal of Sedimentary Petrology*, 59(1), 77-87.

Mcbride, E. F. (1989). Quartz cement in sandstones: a review. *Earth-Science Reviews*, 26(1-3), 69-112.

Morad, S. (1998). *Carbonate cementation in sandstones: controls by patterns of fluid flow and psycho-chemical, environmental and climatic conditions*. Wiley-Blackwell.

Morad, S. (2009). *Carbonate Cementation in Sandstones: Distribution Patterns and Geochemical Evolution*. Blackwell Publishing Ltd.

Morad, S., & De Ros, L.F. (1994). Geochemistry and diagenesis of strata bound calcite cement layers within the Rannoch Formation of the Brent Group, Murchison Field, North Viking Graben (northern North Sea), discussion and reply. *Sedimentary Geology*, 93, 135–147.

Morad, S., Ketzer, J. M., & Ros, L. F. D. (2000). Spatial and temporal distribution of diagenetic alterations in siliciclastic rocks: implications for mass transfer in sedimentary basins. *Sedimentology*, 47(s1), 95-120.

Needham, S.J., 2008. Experimental production of clay rims by macrobiotic sediment ingestion and excretion processes[J]. Journal of Sedimentary Research., 75(6), 1028-1037.

Ozkan, A., Cumella, S. P., Milliken, K. L., & Laubach, S. E. (2011). Prediction of lithofacies and reservoir quality using well logs,

Late Cretaceous Williams Fork Formation, Mamm Creek Field, Piceance Basin, Colorado. AAPG Bulletin, 95(10), 1699-1723.

Pittman, E. D. (1971). Microporosity in carbonate rocks: geological notes. *AAPG Bulletin*, 55.

Pittman, E. D., & Larese, R. E. (1991). Compaction of lithic sands: experimental results and applications. AAPG Bulletin, 75, 8(8), 1279-1299.

Remy, R. R. (1994). Porosity reduction and major controls on diagenesis of Cretaceous-Paleocene volcaniclastic and arkosic sandstone, Middle Park Basin, Colorado. *Journal of Sedimentary Research*, *Section A: Sedimentary Petrology and Processes; (United States)*, 64:4(4), 797-806.

Ros, L. F. D., Anjos, S. M. C., & Morad, S. (1994). Authigenesis of amphibole and its relationship to the diagenetic evolution of Lower Cretaceous sandstones of the Potiguar Rift Basin, Northeastern Brazil. *Sedimentary Geology*, 88(3-4), 253-266.

Ryan, P. C. (1997). The chemical composition of serpentine/chlorite in the Tuscaloosa Formation, United States Gulf Coast: EDX vs. XRD determinations, implications for mineralogic reactions and the origin of anatase. *Clays and Clay Minerals*, 45(3), 339-352.

Shanley, K. W., & Cluff, R. M. (2015). The evolution of pore-scale fluid-saturation in low-permeability sandstone reservoirs. *AAPG Bulletin*, 99(10), 1957-1990.

Sibley, D. F., & Blatt, H., 1976. Intergranular pressure solution and cementation of the tuscarora orthoquartzite. *Journal of Sedimentary Research*, 4, 881-896.

Spoetl, C., Houseknecht, D. W., Longstaffe, F. J. (1994). Authigenic chlorites in sandstones as indicators of high-temperature diagenesis, Arkoma Foreland Basin, USA. *Journal of Sedimentary Research*, 64(3), 553-566.

Stokkendal, J., Friis, H., Svendsen, J. B., Poulsen, M. L. K., & Hamberg, L. (2009). Predictive permeability variations in a Hermod sand reservoir, Stine Segments, Siri Field, Danish North Sea. *Marine & Petroleum Geology*, 26(3), 397-415.

Sullivan, M. D., Haszeldine, R. S., & Fallick, A. E. (1990). Linear coupling of carbon and strontium isotopes in Rotliegend Sandstone, North Sea: Evidence for cross-formational fluid flow. *Geology*, 18(12), 1215-1218.

Surdam, R. C., Boese, S. W., & Crossey, L. J. (1984). The chemistry of secondary porosity. AAPG Memoir, 37(2), 183-200.

Taylor, T. R., Giles, M. R., Hathon, L. A., Diggs, T. N., Braunsdorf, N. R., Birbiglia, G. V., Kittridge M. G., Macaulay, C. I., & Espejo, I. S. (2010). Sandstone diagenesis and reservoir quality prediction: models, myths, and reality. AAPG Bulletin, 94(8), 1093-1132.

Tucker, M.E. (2003). *Sedimentary rocks in the field*. J. Wiley.

Valloni, R., Lazzari, D., & Calzolari, M. A. (1991). Selective alteration of arkose framework in Oligo-Miocene turbidites of the Northern Apennines foreland: impact on sedimentary provenance analysis. *Geological Society London Special Publications*, 57(1), 125-136.

Wang, Q., Zhuo, X. Z., Chen, G. J., & Li, X. Y. (2007). Characteristics of carbon and oxygen isotopic compositions of carbonate cements in Triassic Yanchang sandstone in Ordos Basin. *Natural Gas Industry*, 27(10), 28-32.

Worden, R. H., & Barclay, S.A. (2000). Internally-sourced quartz cement due to externally-derived CO2 in sub-arkosic sandstones, North Sea. *Journal of Geochemical Exploration*, 69(00), 645-649.

Worden, R. H., & Morad, S. (2009). *Clay Mineral Cements in Sandstones*. International Association of Sedimentologists.

Worden, R. H., & Morad, S. (2000). *Quartz Cementation in Oil Field Sandstones: A Review of the Key Controversies. Quartz Cementation in Sandstones.* Blackwell Publishing Ltd, pp. 1-20.

Worden, R., & Morad, S. (2003). Clay mineral cements in sandstones: a review of the detrital and diagenetic sources and evolution during burial.

Xie, X. (2016). Provenance and sediment dispersal of the Triassic Yanchang Formation, Southwest Ordos Basin, China, and its implications. *Sedimentary Geology*, 335, 1-16.

Yang, H., Dou, W. T., Liu, X. Y. (2010). Analysis on sedimentary facies of member 7 in Yanchang formation of Triassic in Ordos basin. *Acta Sedimentologica Sinica*, 28, 254-263.

Yang, H., Jinhua, F. U., Wei, X., & Ren, J. (2011). Natural gas exploration domains in Ordovician marine carbonates, Ordos Basin. *Acta Petrolei Sinica*, 32(5), 733-740.

Zou, C. N., Yang, Z., Tao, S. Z., Yuan, X. J., Zhu, R. K., Hou, L. H., Wu, S. T., Sun, L., Zhang, G. S., Bai, B., Wang, L., Gao, X. H., & Pang, Z. L. (2013). Continuous hydrocarbon accumulation over a large area as a distinguishing characteristic of unconventional petroleum: The Ordos Basin, North-Central China. *Earth-Science Reviews*, 126, 358-369.